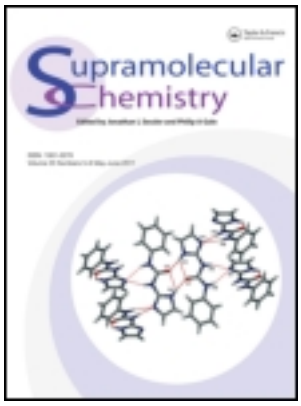

Supramolecular Chemistry
Publication details, including instructions for authors and subscription information:
http://www.tandfonline.com/loi/gsch20

Sulphate binding by a quinolinyl-functionalised tripodal tris-urea receptor

Yongjing Hao [a d], Chuandong Jia [a d], Shaoguang Li [a d], Xiaojuan Huang [a], Xiao-Juan Yang [a], Christoph Janiak [b] & Biao Wu [a c]

[a] State Key Laboratory for Oxo Synthesis and Selective Oxidation, Lanzhou Institute of Chemical Physics, Chinese Academy of Sciences, Lanzhou, 730000, P.R. China

[b] Institut für Anorganische Chemie und Strukturchemie, Universität Düsseldorf, Universitätsstr. 1, D-40225, Düsseldorf, Germany

[c] College of Chemistry and Materials Science, Northwest University, Xi'an, 710069, P.R. China

[d] Graduate University of Chinese Academy of Sciences, Beijing, 100049, P.R. China

Available online: 03 Nov 2011

To cite this article: Yongjing Hao, Chuandong Jia, Shaoguang Li, Xiaojuan Huang, Xiao-Juan Yang, Christoph Janiak & Biao Wu (2012): Sulphate binding by a quinolinyl-functionalised tripodal tris-urea receptor, Supramolecular Chemistry, 24:2, 88-94

To link to this article: http://dx.doi.org/10.1080/10610278.2011.622389

Supramolecular Chemistry
Vol. 24, No. 2, February 2012, 88–94

Sulphate binding by a quinolinyl-functionalised tripodal tris-urea receptor

Yongjing Hao[a,d], Chuandong Jia[a,d], Shaoguang Li[a,d], Xiaojuan Huang[a], Xiao-Juan Yang[a], Christoph Janiak[b] and Biao Wu[a,c]*

[a]*State Key Laboratory for Oxo Synthesis and Selective Oxidation, Lanzhou Institute of Chemical Physics, Chinese Academy of Sciences, Lanzhou 730000, P.R. China;* [b]*Institut für Anorganische Chemie und Strukturchemie, Universität Düsseldorf, Universitätsstr. 1, D-40225 Düsseldorf, Germany;* [c]*College of Chemistry and Materials Science, Northwest University, Xi'an 710069, P.R. China;* [d]*Graduate University of Chinese Academy of Sciences, Beijing 100049, P.R. China*

(*Received 30 June 2011; final version received 7 September 2011*)

A quinolinyl-functionalised tripodal tris(urea) receptor (**L**) has been designed for sulphate binding. The neutral receptor formed the 1:1 binding mode with sulphate ion (as tetrabutylammonium salt). However, when **L** interacted with H_2SO_4, a 2:1 (host/guest) complex $(HL)_2SO_4{\cdot}EtOH{\cdot}12.5H_2O$ (**1**) was isolated. Crystal structural analysis showed that the tertiary amine N atom of **L** is protonated, and the sulphate ion is located outside the receptor rather than inside the tripodal cleft. ^1H NMR studies revealed that the 2:1 binding ratio was persistent in solution. Interestingly, the protonated receptor displayed an unusual enhanced binding for sulphate ion in aqueous environments because of the stronger electrostatic effect in the presence of water.

Keywords: tripodal tris-urea receptor; sulphate binding; quinolinyl; protonation

Introduction

The design of new sulphate receptors continues to be a very active research area because sulphate anion plays many fundamental roles in various biology and environment-related applications such as environmental remediation and nuclear waste cleanup (*1*). In recent years, many sulphate receptors based on macrocycles (*2*), tripodal scaffolds (*3*), podant species (*4*) and metal ion-assisted frameworks have been reported (*5*). However, most of the receptors can only be applied in organic solvents, while in practical applications the binding of sulphate ion in aqueous solutions is required and remains a challenge due to the extremely large hydration energy of sulphate ion ($-1080\,KJ\,mol^{-1}$) (*6*). To overcome the Hofmeister bias, the receptor should have high geometric complementarity, chelation effect and/or hydrophobic effect (*4b*, *6*, *7*). Furthermore, in the anion recognition process, the countercation may have critical impacts on the affinity and selectivity of the receptor (*8*). For instance, the binding of H^+ by some basic groups is an effective way to improve the electrostatic interaction or change the conformation of the receptor by the allosteric effects, thus leading to novel binding behaviour (*8*, *9*).

In previous work, we have studied the anion recognition properties of a series of receptors based on the urea functionality (*3a,b*, *4a,b*, *5a*, *10*). A pyridyl-substituted tripodal tris-urea (L^{py}) has been synthesised, which can selectively encapsulate sulphate ion (*3a*). Recently, we have modified the receptor L^{py} by replacing the pyridyl terminals by the redox-active ferrocenyl groups as an electrochemical reporting unit (L^{Fc}) (*10a*). In the current work, we installed the fluorescent quinolinyl groups to the tripodal tris(urea) backbone to yield the new receptor **L** (Scheme 1), which shows unusual, enhanced binding of the H^+/SO_4^{2-} pair in the presence of water by taking advantage of the electrostatic effect.

Results and discussion

The receptor **L** was synthesised from quinolinyl isocyanate (*11*) and tris(2-aminoethyl)amine (Scheme 1). The crystal structure of **L** forms a 1D chain by six bifurcated intermolecular urea···urea hydrogen bonds around each **L** molecule (Figure 1), which is similar to other known tripodal tris(urea) analogues (*3*). The sulphate compound $(HL)_2SO_4{\cdot}\,EtOH{\cdot}12.5\,H_2O$ (1) was obtained as yellow crystals from **L** and H_2SO_4 in water–ethanol and was characterised by IR spectroscopy, elemental analysis and X-ray crystallography. The anion-binding behaviour of **L** in solution was investigated by ^1H NMR spectroscopy, potentiometric titration and fluorescence methods.

Crystal structure of $(HL)_2SO_4{\cdot}EtOH{\cdot}12.5\,H_2O$ (1)

In the structure of **1**, only the tertiary amine N atom (p*K*a of triethylamine: 10.65) of **L** is protonated, while the three

*Corresponding author. Email: wubiao@nwu.edu.cn

ISSN 1061-0278 print/ISSN 1029-0478 online

http://dx.doi.org/10.1080/10610278.2011.622389
http://www.tandfonline.com

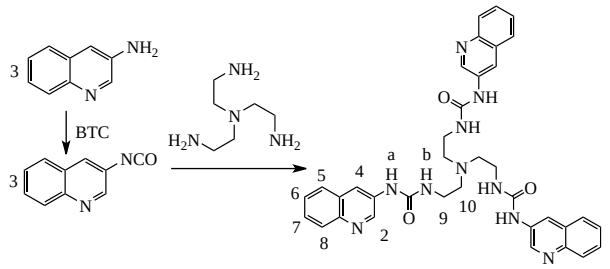

Scheme 1. Synthesis of the receptor **L**.

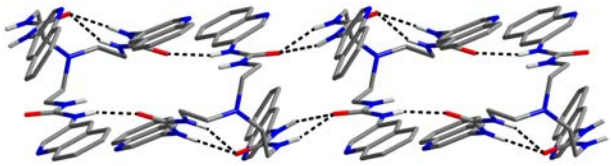

Figure 1. Crystal structure of **L** showing the 1D chain formed by intermolecular urea···urea hydrogen bonds.

quinolinyl N atoms (p*K*a of quinoline: 4.80) (*12*) remain unprotonated. The complex shows a host/guest ratio of 2:1 (HL^+:SO_4^{2-}; Figure 2), which is different from the related ligand L^{py} that formed the complex $[H_4L^{py}(SO_4)_2]$ (*3c*) with both the bridgehead amine and the three pyridyl terminals (p*K*a of pyridine: 5.14) being protonated, thus displaying a host/guest ratio of 1:2 $[(H_4L)^{4+}$:$SO_4^{2-}]$.

Most interestingly, the sulphate ion is located outside the receptor rather than inside the tripodal cleft as in most cases with similar tris(urea) ligands (*3*, *10a*). The protonated amine NH^+ donates a very strong charge-assisted, intramolecular N—H^+···O hydrogen bond to the carbonyl oxygen of one urea arm (N10···O3 = 2.70 Å), and all the NH donors of the three urea arms point outwards, forming hydrogen bonds with sulphate ion or water molecules (Figure 2(a)). This differs from the complex $H_4L^{py}(SO_4)_2$, in which one sulphate ion is encapsulated in the inside of L^{py} and the other remains outside and links adjacent $(H_4L)^{4+}$ units via hydrogen bonding to the pyridinium donors (*3c*). In complex **1**, the S atom of the tetrahedral sulphate ion resides on an inversion centre, and eight half-occupied O atoms define the corners of a cube. Each sulphate ion is bound by two urea arms from two inversion-related **L** molecules and three O—H···O bonds from three surrounding water molecules to make a total of seven contacts (Figure 2(a); N···O/O···O distances ranging from 2.74 to 2.98 Å, and N—H···O/O—H···O angles from 131 to 164°; Table S1 of the Supplementary Information, available online). This anion–receptor arrangement was also found in an adduct of the *t*-Bu-substituted tripodal tris-urea receptor L^{tBu} with $[PtCl_6]^{2-}$, in which the bridgehead N atom is also protonated and the $[PtCl_6]^{2-}$ anion remains between two

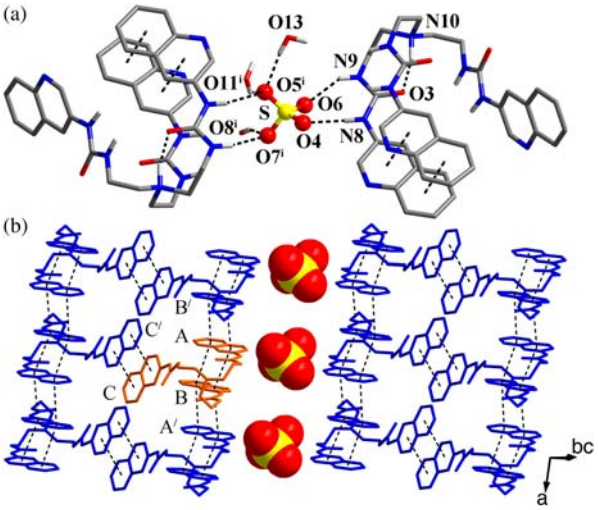

Figure 2. Crystal structure of **1**. (a) Binding of one SO_4^{2-} ion with two LH^+ units. Non-acidic hydrogen atoms were omitted for clarity. Symmetry code: ^{i} 1 − *x*, 1 − *y*, −*z*. (b) Sulphate ions located in the channel formed by **L** with infinite π–π stacking interactions.

receptors (*3e*). Recently, the sulphuric acid complex of a related tripodal tris-urea ligand (the *para*-benzonitrile-substituted analogue), $[HL^{PhCN}\cdot(HSO_4)]$, was reported (*3i*). In contrast to the fully deprotonated H_2SO_4 in the above-mentioned cases with L, L^{py} and L^{tBu}, the acid is deprotonated to hydrogen sulphate (HSO_4^-) which also remains outside the cavity and forms six N—H···O and one O—H···$O_{(C=O)}$ hydrogen bonds with three surrounding mono-protonated ligands. Moreover, in our recent work on the acid complexes of the tris(ferrocenylurea) receptor (L^{Fc}), the bridgehead nitrogen is protonated, while the HSO_4^- anion is similarly located outside the tripodal cavity and anchored by the urea and CH groups of the protonated receptors (*10c*).

There are three π–π stacking interactions in **1**, one intramolecular (between rings A and B; Figure 2(b)) and two intermolecular (A/B′ and C/C′). The dihedral angles of these stacking planes are 6.20°, 6.20°and 0°(A/B, A/B′ and C/C′), and the separations between centroids are 3.77, 4.24 and 4.12 Å, respectively (*13*). These π–π stacking interactions may play crucial roles in the solid-state structure, wherein the sulphate ions are trapped in a channel between the ligands and are protected by the hydrophobic aromatic rings (Figure 2(b)).

^{1}H NMR titration

The anion-binding behaviour of **L** with different anions in solution was investigated by ^{1}H NMR methods. In DMSO-d_6, the urea NH groups displayed large downfield shifts (Δδ: Ha, 1.66; Hb, 2.15 ppm) when 1 equiv. of SO_4^{2-} ions (as Bu_4N^+ salt) was added. No further changes appeared

with more SO_4^{2-}, indicating a 1:1 binding mode which was further confirmed by the results of Job's plot (Figures S3–S5 of the Supplementary Information, available online). The $H_2PO_4^-$, HSO_4^- and OAc^- ions induced smaller downfield shifts in the NH groups ($\Delta\delta$: Ha, 0.76–1.19; Hb, 0.71–1.03 ppm). Notably, the fluoride ion caused a significant downfield shift in the NHa proton ($\Delta\delta$: 1.87 ppm) but much smaller change in the NHb group ($\Delta\delta$: 0.89 ppm), implying that the tripodal scaffold is less complementary for fluoride than for sulphate ion (*3f*, *10a*). Other anions (Cl^-, Br^-, I^-, NO_3^- and ClO_4^-; as Bu_4N^+ salt) resulted in only slight or no changes (Figure S3 of the Supplementary Information, available online). The influence of water to the sulphate binding by **L** was tested. After addition of 25% H_2O, the shifts of the NH signals were greatly recovered ($\Delta\delta$: Ha, 1.14, Hb, 1.62 ppm with 1.0 equiv. of SO_4^{2-}; more water will cause precipitation; Figure 3). This decrease in binding affinity in aqueous environments is normal because water can participate in the competition of the binding process (*6*).

^{1}H NMR studies were also carried out on the binding of **L** with H_2SO_4. When 1.0 equiv. of H_2SO_4 (1.0 M in DMSO) was added to a solution of **L** (20 mM in DMSO-d_6), the urea NH signals showed significant downfield shifts ($\Delta\delta$: Ha, 0.33; Hb, 0.42 ppm). Notably, the NH protons shifted further downfield in the presence of water ($\Delta\delta$: Ha, 0.64; Hb, 0.88 ppm with 25% H_2O), indicating increased binding affinity (Figure 4). The influence of water on the ligand **L** was excluded by control experiments (Figure S6 of the Supplementary Information, available online). To exclude the influence of protonation of the receptor on the NH shifts, the binding of **L** with HNO_3, $HClO_4$ and HCl was tested. Although these acids also caused slight downfield shifts in the NH signals, the addition of water did not lead to further downfield changes or induced upfield shifts (Figures S7–S9 of the Supplementary Information, available online). Thus, the downfield shift under aqueous conditions is unique for sulphate and is due to stronger binding with the anion. Furthermore, most of the protons on the aromatic ring shifted upfield ($\Delta\delta$: -0.18 to -0.55 ppm with 25% H_2O) due to the shielding effect of the $\pi-\pi$ stacking interactions

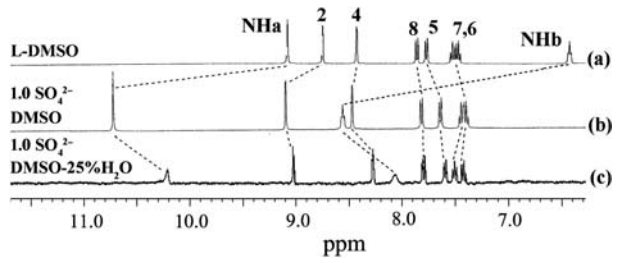

Figure 3. ^{1}H NMR spectra of (a) **L** in DMSO-d_6; (b) **L** + 1.0 equiv. SO_4^{2-} in DMSO-d_6; (c) **L** + 1.0 equiv. SO_4^{2-} in DMSO-d_6–25% H_2O.

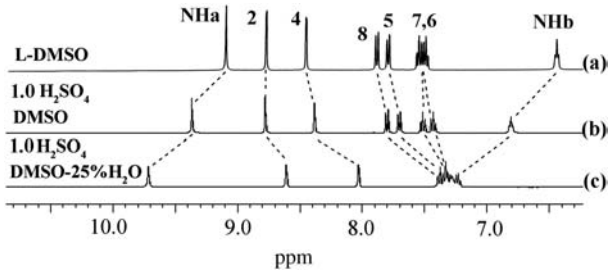

Figure 4. ^{1}H NMR spectra of (a) **L** in DMSO-d_6; (b) L + 1.0 equiv. H_2SO_4 in DMSO-d_6; (c) **L** + 1.0 equiv. H_2SO_4 in DMSO-d_6–25% H_2O.

(Figure 4), while the CH_2 protons moved downfield ($\Delta\delta$: H9, 0.34; H10, 0.81 ppm) upon protonation of the bridgehead amine (Figure S10 of the Supplementary Information, available online). To determine the binding stoichiometry of **L** and H_2SO_4 in solution, Job's plot was performed by NMR spectroscopy (Figure S11 of the Supplementary Information, available online). The results revealed a 2:1 binding mode between **L** and H_2SO_4, which is consistent with the crystal structure and the potentiometric studies (vide infra).

Considering the solid-state structure of **1**, we propose that the unusual enhancement of binding affinity for H_2SO_4 in the highly competitive aqueous environment may be induced by the positive hydrophobic and/or electrostatic effects. To confirm this, two similar model compounds [with pyridyl (L^{py}) and naphthalene (L^{na}) terminals; Scheme S1 of the Supplementary Information, available online] were tested. When 1.0 equiv. of H_2SO_4 was added to L^{py} (to highlight the electrostatic effect, Scheme S1 of the Supplementary Information, available online), the urea NH signals showed some downfield shifts ($\Delta\delta$: Ha, 0.34; Hb, 0.71 ppm), and shifted further in the presence of water ($\Delta\delta$: Ha, 0.51; Hb, 0.99 ppm with 25% H_2O; Figure S12 of the Supplementary Information, available online). For the receptor L^{na} (to highlight the hydrophobic effect, Scheme S1 of the Supplementary Information, available online), the NH signals showed only slight downfield shifts both in pure DMSO ($\Delta\delta$: Ha, 0.18; Hb, 0.21 ppm) and in DMSO–25% H_2O ($\Delta\delta$: Ha, 0.20; Hb, 0.31 ppm; Figure S13 of the Supplementary Information, available online). From these results, it may be concluded that the enhanced binding affinity under aqueous environments is facilitated by both electrostatic effect (accounting roughly 85% based on the chemical shifts) and hydrophobic effect (accounting $\sim$15%), but the former is the major factor because the proton transfer (protonation) may be benefited under aqueous conditions.

Moreover, to elucidate the roles of the nitrogen bridgehead of **L** in the H_2SO_4 binding, a monourea receptor functionalised with quinolinyl group, *N*-phenyl-

N′-(3-quinolinyl)urea (L′), which was previously reported by us (*10b*), was introduced as a simple model. When 1.0 equiv. of H_2SO_4 was added, the urea NH signals of L′ showed some downfield shifts ($\Delta\delta$: Ha, 0.45; Hb, 0.30 ppm). However, the changes were largely recovered in the presence of water ($\Delta\delta$: Ha, 0.19; Hb, 0.07 ppm with 25% H_2O; Figure S14 of the Supplementary Information, available online). These results demonstrate that protonation of the bridgehead nitrogen can provide additional binding affinity through the electrostatic attraction.

Potentiometric studies

The detailed protonation processes of **L** were studied by potentiometric titration in DMSO–25% H_2O (Table S2 and Figure S15 of the Supplementary Information, available online). The first protonation constant (6.64) presumably represents the p*K*a of the amine, which is somewhat smaller than those measured for similar compounds in water (*14*). Then the quinoline groups were protonated, and the values (4.68, 3.99 and 3.84) are also smaller than that in water (p*K*a 4.80) (*12*). The last three protonation processes (mean p*K*a 3.42) might have occurred in the urea carbonyl oxygen atoms (*15*). In addition, the sulphate ion binding of **L** in different protonation states was also investigated by the titration of TBA_2SO_4 (TBA = tetrabutylammonium ion) in the presence of 7 mM $HClO_4$ and 0.05 M (TBA)PF_6 as supporting electrolyte (Table S3 and Figure S16 of the Supplementary Information, available online). In the potentiometric experiments, the monoprotonated species LH^+ showed the largest sulphate-binding constant (log $K = 11.10$), and the value decreased in the following protonation processes (Table S3 and Figure S16 of the Supplementary Information, available online). These potentiometric results are quite unusual compared to the previously described polyamine ligands with multiple protonation states (*16*), in which the higher protonated species have higher binding constant. In the current work, the LH^+ component binds the anion most strongly, which corresponds to the protonation of only the bridgehead amine and is in good agreement with the solid-state structure and Job's plot from ^{1}H NMR data (for the 2:1 LH^+/SO_4^{2-} binding mode). The lower affinities of the higher protonation states observed herein might be explained by the presence of extensive π···π stacking interactions in complex **1** (Figure 2), which would be interrupted when the quinolinyl groups were protonated (in the higher protonation states) due to the electrostatic repulsion (see also the discussion below and Scheme 2).

Fluorescence titration

Initially, the ligand was designed as an optical sensor for anions, so its anion-binding properties were also studied

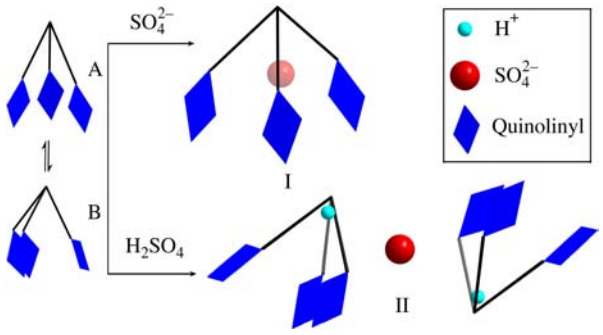

Scheme 2. Proposed binding modes of **L** with SO_4^{2-} and H_2SO_4.

by fluorescence methods. When excited at 335 nm, the free **L** showed the characteristic emission bands of quinoline at 374 and 440 nm. These bands were obviously enhanced upon addition of 1 equiv. of SO_4^{2-} because of the increase in the rigidity of **L** induced by conformational reorganisation upon anion binding. Quantitative investigations of the binding behaviour of **L** with SO_4^{2-} were performed by means of fluorimetric titration in DMSO and DMSO–25% H_2O solutions. The titration profiles point to a 1:1 binding mode between **L** and SO_4^{2-} (Figures 5 and S17 of the Supplementary Information, available online). The association constants (log *K*) calculated by nonlinear fitting of these profiles are 7.02 and 5.88 M^{-1}, respectively (*17*), which agree with the results of ^{1}H NMR study that the binding affinity decreases in the presence of water. Notably, the association constants (log *K*) of **L** with $H_2PO_4^-$, F^-, HSO_4^- and AcO^- in DMSO (6.19, 5.43, 6.00 and 5.66, respectively) do not differ much with SO_4^{2-} (Figures S18–S21 of the Supplementary Information, available online). However, in DMSO–25% H_2O, the

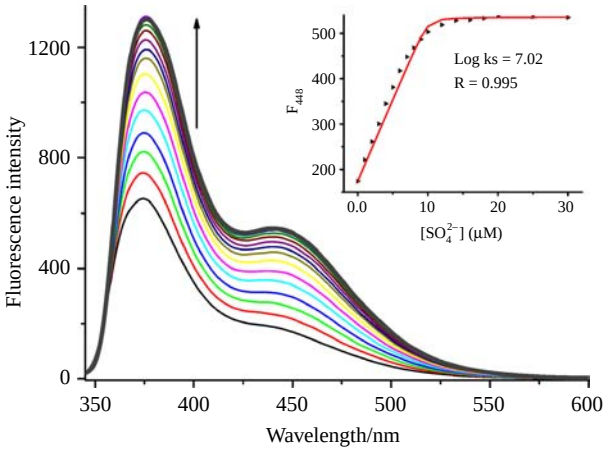

Figure 5. Fluorescence of **L** (10 μM in DMSO) with incremental addition of SO_4^{2-} (up to 30 μM). Excitation wavelength: 335 nm. Inset: variation of the fluorescence of **L** as a function of SO_4^{2-} concentration.

chemosensor **L** can selectively recognise the SO_4^{2-} ion, since other anions only resulted in negligible changes of the fluorescence spectrum in the presence of water (Figure S22 of the Supplementary Information, available online). Similar emission intensity was induced by HSO_4^- under the experimental conditions, which might be due to the conversion of bisulphate to sulphate in DMSO–25% H_2O (*3f*, *10a*). We have also attempted to perform fluorescence titration for H_2SO_4; unfortunately, the changes of the emission spectrum were complicated due to the coexistence of different fluorescence mechanisms and the binding constants could not be calculated from the titration data.

Based on the NMR titration results and the crystal structures of **L** and **1**, it may be possible that the ligand **L** can adopt two fast-exchanging conformations (A and B) in solution (Scheme 2). When SO_4^{2-} anion was added, the neutral receptor **L** tends to assume conformation A. However, in the process of binding with H_2SO_4, it prefers the conformation B by taking the advantage of the π-stacking interactions (*6*, *7a*). The protonation of the bridgehead N atom further promoted this conformational change. The occurrence of the infinite π–π stacking interactions may also explain why only the tertiary amine is protonated and the quinolinyl groups are not in the solid-state structure of **1** even when an excess of H_2SO_4 was used, although the basicity of quinoline (p*K*a 4.80) is very close to pyridine (p*K*a 5.14) (*12*) as mentioned above. The π–π stacking interactions would be disfavoured by the charge repulsion if all the three quinoline groups are protonated (*18*). The change in binding mode was also observed recently in an indole-based anion receptor, wherein the titration curves in pure DMSO were 'less sharp' than those conducted in 10% water (*19*).

Conclusion

In summary, a quinolinyl-functionalised tripodal tris-urea receptor has been designed, which shows an enhanced binding of the H^+/SO_4^{2-} pair in the presence of water. The crystal structure of the H_2SO_4 complex of L, $[(HL)_2SO_4]$ (**1**), reveals a host/guest ratio of 2:1 ($HL^+ : SO_4^{2-}$), in which the bridgehead nitrogen is protonated and the SO_4^{2-} ion is located outside the receptor rather than inside the tripodal cleft. The solid-state structure, ^{1}H NMR and fluorescence studies demonstrate that the electrostatic effect may play a key role in the increased binding of sulphate in aqueous environments.

Experimental section

General

^{1}H and ^{13}C NMR spectra were recorded on a Mercury plus-400 spectrometer with calibration against the solvent signal (DMSO-d_6 2.50 ppm for ^{1}H NMR) or TMS. IR spectra were obtained using a Nicolet AVATAR 360 FT-IR spectrometer as KBr pallets. Elemental analyses were carried out on a VarioEL instrument from Elementaranalysensysteme GmbH. Melting points were detected on an X-4 Digital Vision MP Instrument. Emission spectra were recorded on a Hitachi F7000 fluorescence spectrophotometer equipped with a PX-2 pulsed xenon lamp with an excitation and emission slit width of 2.5 nm. Potentiometric titrations were performed with a PHS-3C precision PH/Mv meter with a combined glass electrode.

Synthesis

*N-[2-[bis[2-[N′-(3-quinolinyl)ureido]ethyl]-amino]ethyl]-N′-(3-quinolinyl)urea (**L**)*

Under nitrogen, 3-aminoquinoline (0.50 g, 3.47 mmol), triphosgene (0.34 g, 1.16 mmol) and triethylamine (0.96 ml, 6.94 mmol) were agitated at ice-cooled conditions in dry CH_2Cl_2 (20 mL). After 2 h, tris(2-aminoethyl)amine (0.17 g, 1.16 mmol) was added. The mixture was stirred for 20 h and then diluted with CH_2Cl_2, washed with H_2O and saturated NaCl and concentrated. The crude product was purified by chromatography (eluent: CH_2Cl_2/MeOH, 20/1 v/v) to yield a white solid (0.41 g, 70%). M.p.: 150–151°C. IR (KBr pellet, cm^{-1}): 3368, 3056, 2970, 1681 (C═O), 1611, 1563, 1248, 747. ^{1}H NMR (DMSO-d_6, 400 MHz): $\delta = 9.08$ (3H, s, Ha), 8.75 (3H, d, $J = 2.4$ Hz, H2), 8.43 (3H, d, $J = 2.4$ Hz, H4), 7.87 (3H, d, $J = 8.0$ Hz, H8), 7.78 (3H, d, $J = 8.0$ Hz, H5), 7.46–7.55 (6H, m, H6,7), 6.43 (3H, t, $J = 5.2$ Hz, Hb), 3.28 (6H, d, $J = 6.4$ Hz, H9), 2.68 (6H, t, $J = 6.4$ Hz, H10). See Scheme 1 for the numbering of the protons. ^{13}C NMR (DMSO-d_6, 100 MHz): $\delta = 155.3$, 144.1, 143.2, 134.3, 128.4, 128.2, 127.1, 126.7, 126.6, 119.3, 53.8 and 37.7. ESI-MS: *m/z* 656.8 $[M + H]^+$. Anal. calcd for $C_{36}H_{38}N_{10}O_4$: C 64.08, H 5.68, N 20.76%; Found: C 63.77, H 5.41, N 20.84%.

*$(HL)_2SO_4$·EtOH·12.5 H_2O (**1**)*

A suspension of **L** (20 mg, 0.030 mmol) in ethanol–water (v/v, 1:1, 2 mL) and a solution of H_2SO_4 (1 M, 60 μL, 0.060 mmol) in water were mixed to give a yellow solution that was allowed to evaporate slowly at room temperature. Yellow crystals were obtained after several days. Yield: 10.1 mg (40%). M.p.: 168–169°C. ^{1}H NMR (DMSO-d_6, 400 MHz): $\delta = 9.36$ (3H, s, Ha), 8.80 (3H, d, $J = 2.4$ Hz, H2), 8.40 (3H, d, $J = 2.4$ Hz, H4), 7.85 (3H, d, $J = 8.4$ Hz, H8), 7.72 (3H, d, $J = 7.6$ Hz, H5), 7.53 (3H, t, $J = 8.0$ Hz, H7), 7.45 (3H, t, $J = 8.0$ Hz, H6), 6.79 (3H, s, Hb), 3.52 (6H, d, $J = 4.8$ Hz, H9), 3.26 (6H, s, H10). IR (KBr pellet, cm^{-1}): 3349, 3088, 2929, 1693 (C═O), 1567, 1369, 1248, 1113 (S—O), 746. Anal. calcd for $(HL)_2SO_4$·12.5 H_2O

($C_{72}H_{105}N_{20}O_{22.5}S$): C 52.78, H 6.10, N 17.10%; Found: C 52.83, H 6.10, N 17.12%.

X-ray crystallography

Diffraction data for the receptor **L** and compound **1** were collected on a Bruker SMART APEX II diffractometer at 173 and 153 K with graphite-monochromated Mo K_α radiation ($\lambda = 0.71073$ Å). An empirical absorption correction using SADABS was applied for all data. The structures were solved by direct methods using the SHELXS program. All non-hydrogen atoms were refined anisotropically by full-matrix least squares on F^2 by the use of the SHELXL program. Hydrogen atoms bonded to carbon and nitrogen were included in idealised geometric positions with thermal parameters equivalent to 1.2 times those of the atom to which they were attached.

*Crystal data for **L***

$C_{37}H_{38}N_{10}O_3Cl_2$ (741.67), colourless block, triclinic, $P-1$, $a = 10.0778(18)$, $b = 12.459(2)$, $c = 15.815(3)$ Å, $\alpha = 105.602(3)°$, $\beta = 94.731(3)°$, $\gamma = 107.147(3)°$, $V = 1799.1(6)$ Å^3, $T = 173(2)$ K, $Z = 2$, $D_c = 1.369$ g/cm^3, $F_{000} = 776$, $\mu = 0.23$ mm^{-1}, 9138 reflections collected, 6308 unique ($R_{int} = 0.033$), no. of observed reflections 5159, $R1 = 0.0645$ ($I > 2\sigma(I)$), $wR2 = 0.252$ (all data). Cambridge Crystallographic Data Centre (CCDC) number: 806486.

*Crystal data for **1***

$C_{37}H_{52.66}N_{10}O_{11.83}S_{0.5}$ (841.42), yellow stick, triclinic, $P-1$, $a = 7.236(2)$, $b = 12.071(4)$, $c = 24.213(8)$ Å, $\alpha = 97.843(4)°$, $\beta = 94.424(4)°$, $\gamma = 96.244(4)°$, $V = 2073.6(12)$ Å^3, $T = 153(2)$ K, $Z = 2$, $D_c = 1.348$ g/cm^3, $F_{000} = 893$, $\mu = 0.13$ mm^{-1}, 12,855 reflections collected, 7097 unique ($R_{int} = 0.066$), no. of observed reflections 2937, $R1 = 0.1354$ ($I > 2\sigma(I)$), $wR2 = 0.4167$ (all data). CCDC number: 806487.

Potentiometric titrations

All potentiometric titrations were performed at room temperature on a PHS-3C precision PH/Mv meter with a combined glass electrode by using TBAOH. The protonation constants were determined from the titration of an approximately 10^{-3} M solution of ligand **L** containing an excess of $HClO_4$ (typically 0.007 M) in the presence of $(TBA)PF_6$ to maintain the ionic strength at 0.05 M. Anion-binding constants for SO_4^{2-} were determined from titrations of an approximately 10^{-3} M solution of **L** containing an excess of $HClO_4$ (typically 0.007 M) in the presence of approximately 0.005 M of $(TBA)_2SO_4$ and $(TBA)PF_6$ (0.05 M) to maintain the ionic strength. The range of accurate pH measurements was considered to be 2.5–11. Stability constants were calculated with the program HYPERQUAD (*20*).

Acknowledgements

This work was supported by the National Natural Science Foundation of China (20872149).

References

(1) Caltagirone, C.; Gale, P.A. *Chem. Soc. Rev.* **2009**, *38*, 520–563.

(2) (a) Sessler, J.L.; Katayev, E.; Pantos, G.D.; Scherbakov, P.; Reshetova, M.D.; Khrustalev, V.N.; Lynch, V.M.; Ustynyuk, Y.A.*J. Am. Chem. Soc.* **2005**, *127*, 11442–11446. (b) Mullen, K.M.; Beer, P.D. *Chem. Soc. Rev.* **2009**, *38*, 1701–1713.

(3) (a) Wu, B.; Liang, J.; Yang, J.; Jia, C.; Yang, X.-J.; Zhang, H.; Tang, N.; Janiak, C. *Chem. Commun.* **2008**, 1762–1764. (b) Zhuge, F.; Wu, B.; Liang, J.; Yang, J.; Liu, Y.; Jia, C.; Janiak, C.; Tang, N.; Yang, X.-J. *Inorg. Chem.* **2009**, *48*, 10249–10256. (c) Custelcean, R.; Bock, A.; Moyer, B.A. *J. Am. Chem. Soc.* **2010**, *132*, 7177–7185. (d) Xie, H.; Yi, S.; Yang, X.; Wu, S. *New J. Chem.* **1999**, *23*, 1105–1110. (e) Warr, R.J.; Westra, A.N.; Bell, K.J.; Chartres, J.; Ellis, R.; Tong, C.; Simmance, T.G.; Gadzhieva, A.; Blake, A.J.; Tasker, P.A.; Schröder, M. *Chem. Eur. J.* **2009**, *15*, 4836–4850. (f) Ravikumar, I.; Lakshminarayanan, P.S.; Arunachalam, M.; Suresh, E.; Ghosh, P. *Dalton Trans.* **2009**, 4160–4168. (g) Stanley, C.E.; Clarke, N.; Anderson, K.M.; Elder, J.A.; Lenthall, J.T.; Steed, J.W. *Chem. Commun.* **2006**, 3199–3201. (h) Custelcean, R.; Remy, P.; Bonnesen, P.V.; Jiang, D.-e.; Moyer, B.A. *Angew. Chem. Int. Ed.* **2008**, *47*, 1866–1870. (i) Pramanik, A.; Thompson, B.; Hayes, T.; Tucker, K.; Powell, D.R.; Bonnesen, P.V.; Ellis, E.D.; Lee, K.S.; Yu, H.; Hossain, M.A. *Org. Biomol. Chem.* **2011**, *9*, 4444–4447.

(4) (a) Jia, C.; Wu, B.; Li, S.; Yang, Z.; Zhao, Q.; Liang, J.; Li, Q.-S.; Yang, X.-J. *Chem. Commun.* **2010**, *46*, 5376–5378. (b) Jia, C.; Wu, B.; Li, S.; Huang, X.; Yang, X.-J. *Org. Lett.* **2010**, *12*, 5612–5615.

(5) (a) Wu, B.; Huang, X.; Xia, Y.; Yang, X.-J.; Janiak, C. *CrystEngComm.* **2007**, *9*, 676–685. (b) Wu, B.; Liang, J.; Zhao, Y.; Li, M.; Li, S.; Liu, Y.; Zhang, Y.; Yang, X.-J. *CrystEngComm.* **2010**, *12*, 2129–2134. (c) Custelcean, R.; Bosano, J.; Bonnesen, P.V.; Kertesz, V.; Hay, B.P. *Angew. Chem. Int. Ed.* **2009**, *48*, 4025–4029. (d) Turner, D.R.; Henry, M.; Wilkinson, C.; McIntyre, G.J.; Mason, S.A.; Goeta, A.E.; Steed, J.W. *J. Am. Chem. Soc.* **2005**, *127*, 11063–11074. (e) Custelcean, R.; Sellin, V.; Moyer, B.A. *Chem. Commun.* **2007**, 1541–1543. (f) Byrne, P.; Lloyd, G.O.; Applegarth, L.; Anderson, K.M.; Clarke, N.; Steed, J.W. *New J. Chem.* **2010**, *34*, 2261–2274.

(6) Kubik, S. *Chem. Soc. Rev.* **2010**, *39*, 3648–3663.

(7) (a) Beer, P.D.; Gale, P.A. *Angew. Chem. Int. Ed.* **2001**, *40*, 486–516. (b) Reyheller, C.; Kubik, S. *Org. Lett.* **2007**, *9*, 5271–5274.

(8) (a) Kim, S.K.; Sessler, J.L. *Chem. Soc. Rev.* **2010**, *39*, 3784–3809. (b) Lloyd, G.O.; Steed, J.W. *Soft Matter* **2011**, *7*, 75–84.

(9) (a) Gale, P.A.; Garric, J.; Light, M.E.; McNally, B.A.; Smith, B.D. *Chem. Commun.* **2007**, 1736–1738. (b) Lakshminarayanan, P.S.; Suresh, E.; Ghosh, P. *Inorg. Chem.* **2006**, *45*, 4372–4380.

(10) (a) Li, M.; Wu, B.; Jia, C.; Huang, X.; Zhao, Q.; Shao, S.; Yang, X.-J. *Chem. Eur. J.* **2010**, *17*, 2272–2280. (b) Jia, C.; Wu, B.; Liang, J.; Huang, X.; Yang, X.-J. *J. Fluoresc.* **2010**, *20*, 291–297. (c) Li, M.; Wu, B.; Cui, F.; Hao, Y.; Huang, X.; Yang, X.-J. *Z. Anorg. Allg. Chem.* **2011**, DOI: 10.1002/zaac.201100214.
(11) Fresneda, P.M.; Molina, P.; Sanz, M.A. *Tetrahedron Lett.* **2001**, *42*, 851–854.
(12) Braude, E.A.; Nachod, F.C. *Determination of Organic Structures by Physical Methods*; Academic Press: New York, 1955.
(13) Janiak, C. *J. Chem. Soc. Dalton Trans.* **2000**, 3885–3896.
(14) Ilioudis, C.A.; Tocher, D.A.; Steed, J.W.*J. Am. Chem. Soc.* **2004**, *126*, 12395–12402.
(15) (a) Hill, C.L.; Bouchard, D.A.; Kadkhodayan, M.; Williamson, M.M.; Schmidt, J.A.; Hilinski, E.F. *J. Am. Chem. Soc.* **1988**, *110*, 5471–5419. (b) Nelyubina, Y.V.; Lyssenko, K.A.; Golovanov, D.G.; Antipin, M.Y. *CrystEngComm.* **2007**, *9*, 991–996. (c) Parkin, A.; Harte, S.M.; Goeta, A.E.; Wilson, C.C. *New. J. Chem.* **2004**, *28*, 718–721.
(16) Bencini, A.; Bianchi, A.; Garcia-España, E.; Micheloni, M.; Ramirez, J.A. *Coord. Chem. Rev.* **1999**, *188*, 97–156.
(17) Valeur, B.; Pouget, J.; Bourson *J. Phys. Chem.* **1992**, *96*, 6545–6549.
(18) Hagihara, Y.; Kataoka, M.; Aimoto, S.; Goto, Y. *Biochemistry* **1992**, *31*, 11908–11914.
(19) Gale, P.A.; Hiscock, J.R.; Jie, C.Z.; Hursthouse, M.B.; Light, M.E. *Chem. Sci.* **2010**, *1*, 215–220.
(20) Gans, P.; Sabatini, A.; Vacca, A. *Talanta* **1996**, *43*, 1739–1753.